Intersubband plasmons in semiconductor quantum wires

G. Y. Hu and R. F. O'Connell
Louisiana State University, Baton Rouge, Louisiana 70803-4001
(Received 28 February 1991)

Intersubband plasmons in semiconductor quantum wires are studied in the harmonic-confinement-potential model and in the random-phase approximation. For a system with M population subbands, we find there exist M different modes of the intersubband plasmon, each of which represents an electronic collective transition from one subband to its adjacent subband. When the coupling between the modes is neglected, an analytic expression for the frequencies of these M modes is derived. Also, we have included the couplings in a numerical calculation. Our calculation shows that, when one increases the magnitude of the gate voltage [such as in the experiments of Hansen *et al.*, Phys. Rev. Lett. **58**, 2586 (1987) and Brinkop *et al.*, Phys. Rev. B **37**, 6547 (1988)], which would effectively increase the subband separation and decrease the Fermi energy, the largest frequency of these multiple intersubband plasmon modes displays a quantum-oscillation behavior but with an overall increasing trend. In addition, the average value over the associated oscillation period for this mode falls in a range that is in good agreement with the experimental observations. Finally, the damping of the intersubband plasmon is analyzed.

I. INTRODUCTION

In a quasi-one-dimensional (Q1D) electronic system, such as the GaAs/$Al_{1-x}Ga_xAs$ quantum wire,[1-3] electrons occupy multiple subbands due to the narrow geometrical dimension ($\sim 10^3$ Å). The typical range of values of the energy separation between these subbands is 1 to 3 meV. The intersubband resonance transition (IRT) plasmon between adjacent Q1D subbands has recently been detected and has attracted a lot of experimental[1-3] and theoretical attention.[4-6]

The current status of the theoretical understanding of IRT plasmons can be best described by mentioning three of the papers[4-6] out of a vast literature. In 1988, Que and Kirczenow[4] presented the first quantum theory of the IRT plasmon and demonstrated explicitly that plasmons with wave vectors perpendicular to the wires can exist in the Q1D regime. Later, Li and Das Sarma[5] showed within the random-phase approximation (RPA) that the depolarization shift correction for the IRT plasmon could be very large, so that the plasmon excitation energy can be significantly higher than the corresponding single-particle excitation energy for realistic experimental conditions. Good qualitative and semiquantitative agreement[5] with experimental results is reached. Both papers have the "few-subband-approximation" restriction, i.e., a 2- or 3-subband model is used in the calculation (whereas the actual system used in the experiments has about 5–10 subbands populated). Thus, we are motivated to study multisubband IRT plasmon modes. Also, one of the key observations from the experiments, the increase of the IRT plasmon excitation energy with decreasing electron density (or Fermi energy), remains unexplained *from the point of view of the collective excitation.* Recently, we have presented a theory[6] which studies the Q1D system without implementing the "few subband approximation." In our treatment, the main obstacle in studying the multisubband Q1D system, the electron-electron (e-e) interaction matrix, is removed by a clear analysis in the harmonic-confinement potential model. In the literature,[4-6] Q1D systems are generally studied using a hard-wall potential-well confinement (where the subband energy $\varepsilon_n \propto n^2$), or else a harmonic-confinement potential ($\varepsilon_n \propto n$). Detailed self-consistent numerical work by Laux and Stern[7] shows that the actual confining potential is somewhat in between. The obvious advantage to the use of the harmonic-confinement potential used here is to make an analytic analysis possible. We will comment later that the qualitative results remain the same in both models. The focus of our previous paper[6] is the evaluation of the e-e interaction matrix, and a preliminary application to the study of the IRT plasmon shows that our theory is in good agreement with most aspects of the experimental observation in the first-order approximation (neglecting the coupling between different IRT plasmon modes). In this paper, we give a comprehensive study of the density dependence for the frequency of the IRT plasmon. Also, the coupling between the IRT plasmons is considered. Our results include a full analysis of the structure of the IRT plasmon between adjacent Q1D subbands and the finding of a quantum-oscillation phenomenon for the IRT plasmon frequencies (as a function of the electron density).

In Sec. II, starting with the determinant equation for the physical excitation energies of the Q1D system for an M populated subband system, we show that a relatively simple result ensues when the coupling between the IRT plasmon modes is neglected (and we demonstrate that the higher the subband index the less important is such coupling). However, such coupling is included in a numerical study which we have carried out. In Sec. III we study the magnitude of the damping of the plasmon mode. Finally in Sec. IV we compare our results with experiments and discuss our conclusions.

II. INTERSUBBAND RESONANCE TRANSITION PLASMONS

The physical excitation energies of the Q1D system are obtained from the determinant equation[5,6]

$$\det[\epsilon(q,\omega)]=0 , \tag{1}$$

where $\epsilon(q,\omega)$ is the dielectric matrix function. Previously[6] we have worked out the form of $\epsilon(q\to 0,\omega)$ in the RPA approximation and by using the harmonic-confinement potential model, where one assumes the electrons are in an xy plane with negligible thickness and a lateral quantized subband energy $\varepsilon_n=(n+\frac{1}{2})\hbar\omega_0$, with $n=0, 1, 2,\ldots$ and ω_0 the characteristic frequency. Here, all the Q1D wires in the xy plane are assumed to have the same constant width, i.e., we neglect fluctuations of the width due to inhomogeneity of the gates. However, inhomogeneity effects on the IRT plasma frequency are discussed in the concluding section.

According to Ref. 6, the contributions of the relevant matrix elements in (1) to the calculation of the energies associated with the IRT plasmons between the adjacent levels are (with $|i-j|=1$),

$$\epsilon_{ij,ij}(q=0,\omega)=1-\frac{2C_i}{\omega+(i-j)\omega_0} , \tag{2a}$$

$$\epsilon_{ji,ij}(q=0,\omega)=-\frac{2C_i}{\omega+(i-j)\omega_0} , \tag{2b}$$

$$\epsilon_{ij,lm}(q=0,\omega)=-\frac{1}{(i!j!l!m!)^{1/2}}\frac{2C_i}{\omega+(i-j)\omega_0} , \quad l \text{ or } m\neq i,j \tag{2c}$$

where

$$C_i=\frac{2b^2}{\pi a_B^*}(k_{Fi}-k_{Fj}) , \tag{2d}$$

and where $b=(\hbar/m^*\omega_0)^{1/2}$, m^* is the effective mass, $k_{Fi}=[2m^*(\varepsilon_F-i\hbar\omega_0)/\hbar^2]^{1/2}$ except that $k_{Fi}=0$ if $\varepsilon_F<i\hbar\omega_0$, and ε_F is the Fermi energy measured from the zero-point energy $\frac{1}{2}\hbar\omega_0$.

Using (2), after some algebra one deduces from (1) the determinant equation which determines the IRT plasmon for an M-populated subband system,

$$\begin{vmatrix} \gamma^2-1-2C_0 & -\sqrt{2}C_0 & \cdots & -\dfrac{2C_0}{(M-1)!\sqrt{M}} \\ -\sqrt{2}C_1 & \gamma^2-1-2C_1 & \cdots & -\dfrac{2C_1}{(M-1)!\sqrt{2M}} \\ \vdots & \vdots & & \vdots \\ -\dfrac{1C_{M-1}}{(M-1)!\sqrt{M}} & -\dfrac{2C_{M-1}}{(M-1)!\sqrt{2M}} & \cdots & \gamma^2-1-2C_{M-1} \end{vmatrix} , \tag{3}$$

where $\gamma\equiv\omega/\omega_0$ and C_i is defined by (2d). We note that in Ref. 6 we have shown that the IRT plasmon is rigorously decoupled from the intrasubband plasmon as long as the confinement potential is laterally symmetric. Also we note that the structure of the off-diagonal elements shows that the higher the subband index, the less important is the coupling between the different IRT plasmon modes.

When the coupling between the IRT plasmon modes is neglected [neglecting the off-diagonal elements in (3)], the IRT plasmon frequencies ω_p for a system with M-populated subbands can be directly obtained from (3) as

$$\gamma_i\equiv\frac{\omega_p^{i+1}}{\omega_0}=\left[1+\frac{4b^2}{\pi a_B^*}(k_{Fi}-k_{Fi+1})\right]^{1/2} , \quad i=0,1,\ldots,M-1 . \tag{4}$$

A few comments on (4) are in order. First, there exists M different modes of intersubband plasmons for an M-populated subband system, each representing an electronic collective transition from one subband to its adjacent subband. In addition, one observes that $\gamma_0<\gamma_1<\cdots<\gamma_{M-2}$, as $k_{Fi}-k_{Fi+1}$ becomes larger for smaller values of i [except for $i=M-1$, where $k_{F,M-1}-k_{FM}$ depends only on the population of the $(M-1)$th subband]. Second, we will show in the following section that among the M different modes, the mode which has the largest value of $(k_{Fi}-k_{F,i+1})$ in (1) has the smallest damping, and is likely the dominant mode being detected by the experiments. Third, from (4) it follows that the dominant mode is either the ω_P^M mode [when the $(M-1)$th subband is *significantly filled*] or the ω_p^{M-1} mode [when the $(M-1)$th subband is almost empty]. When the ω_p^M mode dominates we see from (4) and the fact that $k_{FM}=0$ that the plasmon energy increases with an increase of the Fermi energy. When the ω_p^{M-1} mode dominates one can show from (4) that the plasmon energy decreases with the increase of the Fermi energy. Thus, based on the above comments one observes that when the magnitude of the gate voltage is increased so as to effectively increase ω_0 and decrease ε_F, the plasmon energy displays both an increasing behavior (when the ω_p^{M-1} mode dominates), and a decreasing behavior (when the ω_p^M mode dominates), in consecutive order, but the overall trend is an increasing behavior.

The basic feature described above for the intersubband plasmon of an ideal Q1D electron system remains when the mode coupling (the off-diagonal elements) is included by solving (3). In the following we first study the two-modes case analytically, and then the many-modes (more

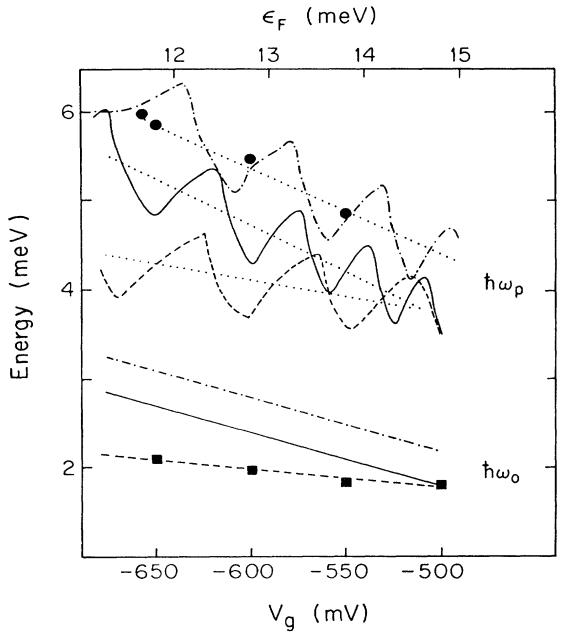

FIG. 1. Intersubband plasmon energy $\hbar\omega_p$ as a function of the gate voltage V_g (the corresponding linear scale of the Fermi energy of the upper axis is chosen by fitting to the experimental data of Ref. 1). Results are presented for three sets of $\hbar\omega_p$ (upper part) calculated at the corresponding different values of the subband separations $\hbar\omega_0$ (lower part). Dotted lines represent the values of $\hbar\omega_p$ averaged over its associated periods. Solid squares and circles are the parameters given by Ref. 1, as deduced from the experimental data.

than two) case numerically followed by a direct comparison with the experimental data.

When the Q1D system is populated only to the two lowest subbands, there can only be two different IRT plasmon modes. In this case (3) reduces to its top left 2×2 matrix, the solution of which can easily be obtained as

$$\gamma_\pm \equiv \omega_p^\pm/\omega_0 = [1+C_0+C_1 \pm (C_0^2+C_1^2)^{1/2}]^{1/2} . \quad (5)$$

Equation (5) shows that the coupling of the two modes is not important when $C_1 \to 0$ (the population of the first subband tends to zero) in which case $\gamma_0=\gamma_+\approx\sqrt{1+2C_0}$ and $\gamma_1=\gamma_-\approx 1$. They are strongly coupled when C_0 and C_1 are comparable, which pushes the higher-frequency mode (here $\gamma_1=\sqrt{1+2C_1}$)toward the higher coupled mode γ_+ and the lower-frequency mode (here $\gamma_0=\sqrt{1+2C_0}$ toward the lower coupled mode γ_-. For example, it is straightforward to obtain $\gamma_+\approx\sqrt{1+3C_1}$ from (5) when $\epsilon_F=2\hbar\omega_0$.

This coupled IRT plasmon modes picture can directly be extended to a Q1D system with M-populated subbands, where the original M IRT plasmon modes are coupled into M new modes possessing different frequencies than the uncoupled ones. On the other hand, as the mode involved with higher subband index i has smaller coupling [see the off-diagonal elements in Eq. (3)], the IRT plasmons in the many-subbands system is not just a simple extended picture of the $M=2$ case. In other words, to obtain an accurate analysis of the multiple IRT plasmons, one should solve (3) exactly. In Fig. 1, we present our numerical solution of (3) for the dominant mode of the IRT plasmons, where the values of M (5–10) and ω_0 (1–3 meV) are chosen in the range comparable to that of the experiments. The figure shows that when one increases the magnitude of the gate voltage as to effectively increase ω_0 and decrease ϵ_F, the IRT plasmon energy displays both an increasing behavior (when the ω_p^{M-1} mode dominates) and a decreasing behavior (when the ω_p^M mode dominates) in consecutive order, but the overall trend is an increasing behavior.

III. DAMPING OF THE IRT PLASMONS

In the preceding section we have shown that there exists M different IRT plasmon modes for a system with M-populated subbands. Also, we have stated that the mode with the largest frequency has the smallest damping and is more likely the dominant mode detected by the experiments. In this section we prove the above statement by studying the frequency (ω) dependence of the imaginary part of the intersubband density-response function $\mathrm{Im}\chi^0_{nn'}(q,\omega)$, which is known to be directly proportional to the magnitude of the damping of the plasmon mode.

$$\mathrm{Im}\chi^0_{nn'}(q,\omega) = -\pi \sum_k (f_{nk}-f_{n',k+q})\delta(\omega-\epsilon_{n',k+q}+\epsilon_{nk}) , \quad (6)$$

where $\epsilon_{nk}=\epsilon_n+\hbar^2k^2/2m^*$, and the Fermi distribution function $f_{nk}=(e^{\beta(\epsilon_{nk}-\epsilon_F)}+1)^{-1}$. After making the transform $\sum_k \to (2/2\pi)\int dk$ and after some straightforward algebra, we obtain

$$\mathrm{Im}\chi^0_{nn'}(q,\omega) = \frac{m^*}{q}[(e^{\beta(m^*/2v_+^2-\epsilon_{Fn'})}+1)^{-1} - (e^{\beta(m^*/2v_-^2-\epsilon_{Fn})}+1)^{-1}] , \quad (7)$$

where

$$v_\pm = \frac{\omega-\omega_0}{q}+\frac{\hbar q}{2m^*} . \quad (8)$$

We note that, at $T=0$, (7) reduces to

$$\mathrm{Im}\chi^0_{nn'}(q,\omega) = \frac{m^*}{q}\left[\Theta\left[1-\frac{v_+^2}{v_{Fn'}^2}\right]-\Theta\left[1-\frac{v_-^2}{v_{Fn}^2}\right]\right] , \quad (9)$$

which agrees with our previous work[8] for the $T=0$ density-response behavior of the Q1D system.

Equation (7) tells us that at $T\neq0$, all the IRT plasmons are more or less damped, as $\mathrm{Im}\chi^0_{nn'}(q\omega)$ is nonvanishing. Also from (7) it is straightforward to show that

$$\frac{\partial}{\partial\omega}\mathrm{Im}\chi^0_{nn'}(q\to0,\omega)<0 , \quad (10)$$

which implies that the larger the plasmon frequency the smaller the damping it has.

IV. CONCLUSIONS

We have studied the intersubband plasmons of Q1D systems in the harmonic-confinement-potential model and in the RPA approximation. For a system with M-populated subbands, we find there exists M different modes of the intersubband plasmon, each of which represents an electronic collective transition from one subband to its adjacent subband. Our calculation shows when one increases the magnitude of the gate voltage so as to effectively increase the subband separation and decrease the Fermi energy, the largest frequency of these multiple intersubband plasmon modes displays a quantum-oscillation behavior but with an overall increasing trend. Also, our analysis of the damping of the intersubband plasmon modes at finite temperatures demonstrates that the largest frequency mode has the smallest damping and is the dominant mode being detected by experiments.

The actual value of the ω_0 and the electron density may be slightly different for each individual wire in the sample. Therefore, we propose that the actual measured $\hbar\omega_p$ in the experiments of Hansen *et al.*[1] (whose one-dimensional multiwire structures contained $\approx 10^4$ wires) corresponds to the averaged value of $\hbar\omega_p$ (dotted line) shown in that figure. On the other hand, our results do imply that the quantum-oscillation behavior discussed here should be observable for an ideal sample.

We note that the above conclusions should be model independent even though we have confined our discussion to the harmonic-potential model. In fact, it is not difficult to see that when a different model, such as the hard-wall potential, is used in the calculation, the only change in the RPA formalism of the dielectric function is the Fourier component of the Coulomb interaction. It follows that when a different model is used in our calculation of the RPA dielectric function at $q=0$, only the form of the prefactor $2b^2/\pi a_B^*$ for C_i in Eqs. (2) and (3) will be different, while the k_{Fi} and ω dependence is unchanged. As a result, the qualitative feature for the $q=0$ IRT plasmon discovered in this paper holds for any other model for the confinement potential. The advantage of using the harmonic-confinement potential is that it is a model very close to the real situation, and it makes the analytic analysis (2)–(4) possible.

Finally, we mention that there appeared recently another point of view[9] which interprets the results of Ref. 1 as a single-particle intersubband transition behavior, which is obviously distinct from the collective excitation picture presented in this paper. According to this single-particle picture, the detected transition energy simply corresponds to the value of the bare harmonic potential at that specific gate voltage, and the change of the transition energy at different gate voltages is solely due to the change of the bare confinement potential. The arguments for this picture depend strictly on the assumption of the harmonic-confinement potential. Within this view, one certainly will not see any quantum oscillation for the intersubband transition energy since it is no longer a density-dependent quantity. Also, there is only one mode no matter how many subbands are populated. The multimodes and the quantum-oscillation phenomena predicted in this paper in the collective excitation picture provides a clear difference between the predictions of the single-particle and the collective excitation pictures.

In our view the correctness of either the single-particle picture or the collective excitation picture may eventually be checked by experiments in at least two ways. One way is to detect the change of the intersubband transition energy by changing either the electron density or the confinement potential but not both of them. In this way, there will be no ambiguity as to the key factor affecting the change of the intersubband transition energy. For example, in Ref. 10, Ismail, Antoniadis, and Smith measured the conductance for a multiparallel semiconductor quantum wire by changing the electron density while the confinement potential is fixed. It will be interesting to see the experimental results for the intersubband transition energy using a similar procedure.

The other way is to improve the homogeneity of the sample so as to reduce the width variation of the quantum wires. From (4) one can roughly estimate (see Fig. 1) that the amplitude of the plasmon oscillation is in the order of $0.2\omega_0$. If the variation of the wires' width can be controlled within a small range, say $0.1\omega_0$, then the plasmon quantum oscillation will not be smeared out by the inhomogeneity and therefore will be detectable. We hope the theory presented here will stimulate more experimental interest.

ACKNOWLEDGMENTS

The work was supported in part by the U.S. Office of Naval Research under Grant No. N00014-90-J-1124.

[1] W. Hansen, M. Horst, J. P. Kotthaus, U. Merkt, Ch. Sikorski, and K. Ploog, Phys. Rev. Lett. **58**, 2586 (1987); F. Brinkop, W. Hansen, J. P. Kotthaus, and K. Ploog, Phys. Rev. B **37**, 6547 (1988).

[2] T. Demel, D. Heitmann, P. Grambow, and K. Ploog, Phys. Rev. B **38**, 12 732 (1988).

[3] T. P. Smith III, J. A. Brum, J. M. Hong, C. M. Knoedler, H. Arnot, and L. Esaki, Phys. Rev. Lett. **61**, 585 (1988).

[4] W. Que and G. Kirczenow, Phys. Rev. **37**, 7153 (1988).

[5] Qiang Li and S. Das Sarma, Phys. Rev. B **40**, 5860 (1989).

[6] G. Y. Hu and R. F. O'Connell, Phys. Rev. B **42**, 1290 (1990).

[7] S. Laux and F. Stern, Appl. Phys. Lett. **49**, 91 (1986).

[8] G. Y. Hu and R. F. O'Connell, J. Phys. Condens. Matter **2**, 9381 (1990).

[9] J. P. Kotthaus, in Physics of Granular Nanoelectronics, edited by D. K. Ferry, J. Barker, and C. Jacobini (Plenum, New York, in press).

[10] K. Ismail, D. A. Antoniadis, and H. I. Smith, Appl. Phys. Lett. **54**, 1130 (1989).